SLAC-PUB-9356
August 2002

STUDY OF INTRABEAM SCATTERING IN LOW-ENERGY ELECTRON RINGS

Marco Venturini*
Stanford Linear Accelerator Center, Stanford University, Stanford, CA 94309 USA

Abstract

The paper contains a study of intrabeam scattering in a low energy electron storage ring to be used as part of a Compton back-scattering x-ray source. We discuss time evolution of emittances and dependence of IBS growth rates on lattice parameters.

1 INTRODUCTION

Practical use of Compton back-scattering for x-ray production has been suggested by several authors. Recently Z. Huang and R. Ruth [1] proposed a novel scheme that involves the interaction between a laser pulse trapped in an optical cavity and a fast recirculating electron bunch. The proposal is currently being considered for implementation.

The size of the required storage ring is naturally small (to boost the electron-photon collision rate) and the energy low. Production of x-rays of the order of 1 Å– a value of interest in many applications – using a 1 μ wavelength laser requires an electron energy of only about 25 MeV. While appealing for obvious reasons such a low value for the energy gives the machine performance the unusual feature of being limited by intrabeam scattering (IBS). Relatively low emittances in all three degrees of freedom are desired to achieve acceptably high brightness. Transverse (normalized) emittances and relative momentum spread should be of the order of $10^{-6} - 10^{-5}$ m and 10^{-3} respectively for a given reasonable choice of the other relevant parameters ($N = 6 \times 10^9$ particles/bunch, 1 cm rms bunch length, $\beta_x^* \simeq \beta_y^* \simeq 1$ cm at interaction, 3 m ring circumference and 3 mJ laser pulse energy in the optical cavity). With these phase-space dimensions the IBS growth time is a few msecs, much shorter than the radiation damping time due to either synchrotron light or x-ray emission (which are of the order of 1 sec). The goal of this study is to carry out a detailed calculation of the IBS growth rates for a realistic lattice and determine an adequate value for the repetition rate necessary to maintain acceptable beam quality.

2 IBS THEORY

An IBS theory can be built on two basic assumptions: i) particles undergo random and uncorrelated collisions ii) collisions are properly described by the Rutherford cross section. On this basis one can derive a diffusion equation with drift and diffusion coefficients depending on the beam distribution [3]. By making additional assumptions on the form of the beam distribution one can then derive

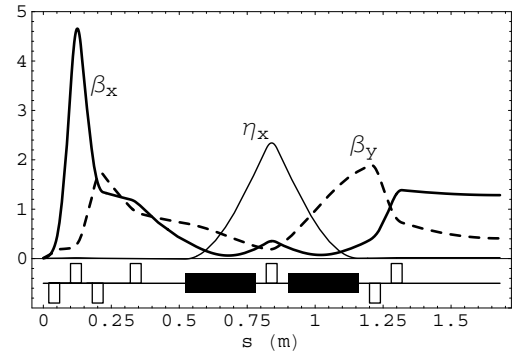

Figure 1: Lattice functions; β–functions are in m, η_x is in units of 10 cm.

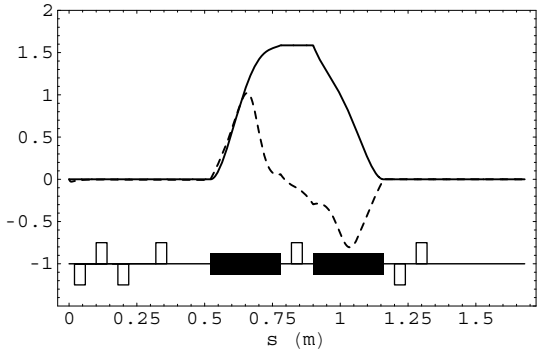

Figure 2: Lattice function $\mathcal{H}_x$ (solid line) in units of 10 cm and ϕ_{Bx} (dimensionless).

expressions for the emittance growth rates. This is done in [2] for gaussian beams. The two theories by Bjorken-Mtingwa (BM) and Piwinski are basically equivalent – except for some different approximations employed. In this study we mostly used the BM formulation – a part from occasional comparisons with Piwinski's. BM expressions for the growth rates of the transverse (unnormalized) rms emittances $\tau_x^{-1} = \varepsilon_x^{-1} d\varepsilon_x/dt$, $\tau_y^{-1} = \varepsilon_y^{-1} d\varepsilon_y/dt$ and relative momentum spread $\tau_p^{-1} = {\sigma_p}^{-1} d\sigma_p/dt$ for a bunch of N charged particles with relativistic factor γ_0 can be written in the form

$$\frac{1}{\tau_x} = \langle \frac{\mathcal{H}_x}{\varepsilon_x}\gamma_0^2 I_{zz} - 2\frac{\beta_x\phi_{Bx}}{\varepsilon_x}\gamma_0 I_{xz} + \frac{\beta_x}{\varepsilon_x} I_{xx}\rangle_s, \quad (1)$$

$$\frac{1}{\tau_y} = \langle \frac{\mathcal{H}_y}{\varepsilon_y}\gamma_0^2 I_{zz} - 2\frac{\beta_y\phi_{By}}{\varepsilon_y}\gamma_0 I_{yz} + \frac{\beta_y}{\varepsilon_y} I_{yy}\rangle_s, \quad (2)$$

$$\frac{1}{\tau_z} = \langle \frac{1}{2}\frac{\gamma_0^2}{\sigma_p^2} I_{zz}\rangle_s. \quad (3)$$

* venturin@slac.stanford.edu

Work supported by the Department of Energy contract DE-AC03-76SF00515.

where ϕ_{Bi} is the function $\phi_{Bi} = \eta_i' + \alpha_i \eta_i / \beta_i$ and α_i, β_i, γ_i and η_i are the usual lattice and dispersion functions in the horizontal ($i = x$) and vertical ($i = y$) plane. The integrals

$$I_{ij} = A \int_0^\infty d\lambda \frac{\lambda^{\frac{1}{2}}}{\sqrt{\det \Lambda}} (\delta_{ij} \mathrm{Tr} \Lambda^{-1} - 3\Lambda_{ij}^{-1}), \quad (4)$$

are defined in terms of the matrix $\Lambda = \mathbf{1}\lambda + \mathrm{L}$, with

$$\mathrm{L} = \begin{bmatrix} \frac{\beta_x}{\varepsilon_x} & 0 & -\gamma_0 \frac{\beta_x \phi_{Bx}}{\varepsilon_x} \\ 0 & \frac{\beta_y}{\varepsilon_y} & -\gamma_0 \frac{\beta_y \phi_{By}}{\varepsilon_y} \\ -\gamma_0 \frac{\beta_x \phi_{Bx}}{\varepsilon_x} & -\gamma_0 \frac{\beta_y \phi_{By}}{\varepsilon_y} & \frac{\gamma_0^2 \mathcal{H}_x}{\varepsilon_x} + \frac{\gamma_0^2 \mathcal{H}_y}{\varepsilon_y} + \frac{\gamma_0^2}{\sigma_p^2} \end{bmatrix}$$

where ($i = x, y$), $\mathcal{H}_i = \beta_i \eta_i^{'2} + 2\alpha_i \eta_i \eta_i' + \gamma_i \eta_i^2$. The constant $A = c r_c^2 N \log \Lambda_c / (8\pi \beta_0^3 \gamma_0^4 \varepsilon_x \varepsilon_y \sigma_p \sigma_s)$ involves the classical radius of the particle r_c, the rms bunch length σ_s, the relativistic factor β_0 and the so-called Coulomb logarithm with $\Lambda_c \simeq 2/\theta_m$. In emittance dominated beams the minimum Coulomb scattering angle θ_m is determined by bunch sizes. We set $\log \Lambda_c = 16$. The quantities on the RHS of (1)-(3) are understood to be averaged $\langle \cdots \rangle_s$ along the lattice. The following calculations were carried out using the specifically written Mathematica package *Math-Lattice*. The package (based in part on the package SynchrotronDesign [4] for determining the lattice functions) computes the integrals (4) efficiently using the Mathematica built-in functions. When the eigenvalues of L are non-degenerate (degenerate) the integrals (4) reduce to combinations elliptical integrals (elementary functions). Close to degeneracy the integrals are most accurately evaluated from their Taylor expansion in the differences of the eigenvalues.

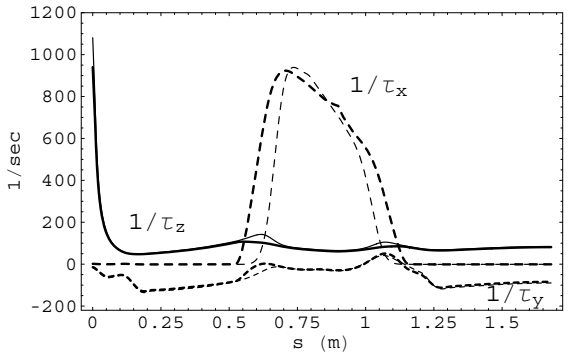

Figure 3: Local IBS growth rates along the lattice. Thick lines refer to calculation done according to Bjorken-Mtingwa; thin lines are calculated according to Piwinski. The vertical growth rate $1/\tau_y$ is magnified by a factor 100.

3 DISCUSSION

The present discussion will be mostly based on the case-study lattice shown in Figs. 1 and 2 (the two pictures are relative to half lattice). The lattice has a two-fold symmetry and includes four 90^0 bends and 14 quads for a total length of 3.36 m. The tunes are $\nu_x = 2.36$ and $\nu_y = 1.40$. Dispersion is suppressed in the two main straight sections to accommodate injection elements and an RF cavity on the one side and interface with the optical cavity on the other. At the IP ($s = 0$) with the laser pulse the betatron functions have the values $\beta_x^* = 0.86$ cm and $\beta_x^* = 0.99$ cm. In the IBS calculations we included no errors and in particular no vertical dispersion (*i.e.* $\mathcal{H}_y = \phi_{By} = 0$). As a result of the absence of coupling with the longitudinal motion the IBS growth rate in the vertical plane τ_y^{-1} is about two order of magnitudes smaller than τ_x^{-1} and τ_z^{-1}. See Fig 3. Under the assumption that the bunch distribution remains gaussian in all three degrees of freedom one can use equation (1)-(3) for the growth rates to evaluate the emittance and relative momentum spread over time. The bunch length is related to the relative momentum spread by $\sigma_s(t) = \sigma_{s0} \sigma_p(t) / \sigma_{p0}$, with $\sigma_{s0} = \sigma_s(0)$ and $\sigma_{p0} = \sigma_p(0)$.

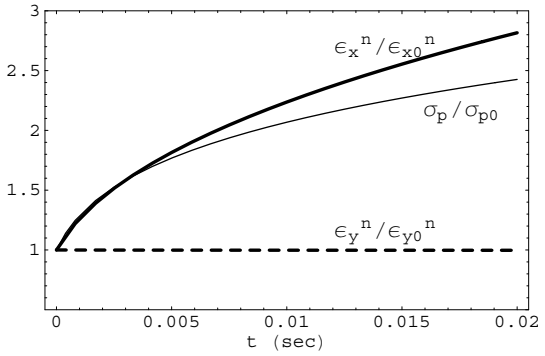

Figure 4: Evolution of (normalized) rms emittances (in m) and relative momentum spread. $E = 25$ MeV.

Table 1: Evolution of emittances and momentum spread. Initial values: $\varepsilon_{x0}^n = \varepsilon_{y0}^n = 5\mu$, $\sigma_{p0} = 10^{-3}$.

	t=0.016 sec			**t=0.008 sec**		
E (MeV)	**18**	**25**	**36**	**18**	**25**	**36**
ε_x^n (μ)	13.5	13.2	12.7	10.8	10.6	10.1
ε_y^n (μ)	4.97	4.98	4.99	4.98	4.99	4.99
σ_p (10^{-3})	2.66	2.32	2.00	2.26	1.98	1.7

In the calculation radiation effects can be neglected because, as already pointed out, the corresponding damping time is much longer than the IBS time scale. An example of solution with initial conditions $\varepsilon_{x0}^n = \varepsilon_{y0}^n = 5\ \mu$, $\sigma_{p0} = 10^{-3}$ is shown in Fig. 4. Other relevant parameters are $N = 6 \times 10^9$, $\sigma_{s0} = 1$ cm, $E = 25$ MeV. One can see that over an interval of 20 msec the vertical emittance remains unchanged while the horizontal emittance and momentum spread increase by about a factor 3 and 2.5 respectively. Intermediate changes at $t = 0.0166$ and $t = 0.008$ sec corresponding to repetition rates of 60 and 120 Hz are reported in Table 1. Because the storage ring should function over a range of energies to allow tunability of the x-ray source, the calculation has been repeated for $E = 18$ MeV and $E = 36$ MeV – which define an interval of interest in applications like, for example, protein crystallography. The

results are also reported in Table 1.

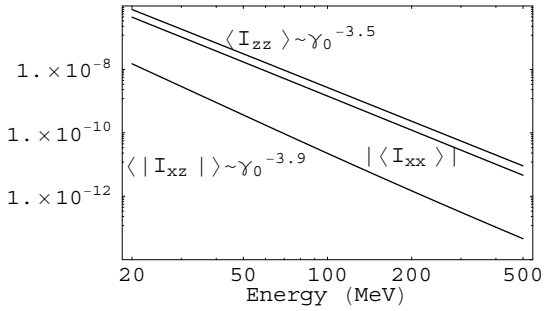

Figure 5: Scaling of the s-averaged integrals I_{ij} with respect to the beam energy for $\varepsilon_x^n = \varepsilon_y^n = 5\ \mu$, $\sigma_p = 2 \times 10^{-3}$.

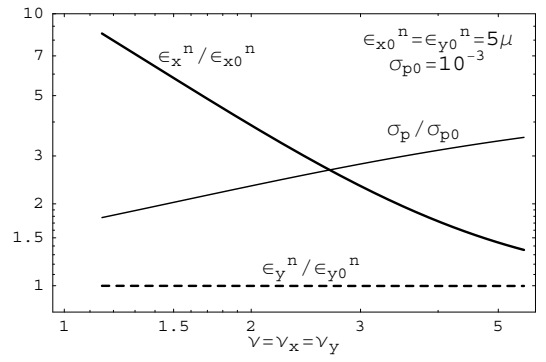

Figure 6: Emittances and relative momentum spread deviation as functions of tune after $t = 0.0166$ sec. Lattice treated in the smooth approximation.

An interesting question concerns the possibility of controlling the effect of IBS by an appropriate design of the lattice. Let us take a closer look at Eqs. (1)–(3) and single out the relevant terms. First observe that the s-averaged integral expressions $\langle I_{xx}\rangle_s$ and $\langle I_{zz}\rangle_s$ have about the same order of magnitude for values of the emittances falling in our range of interest, see Fig. 5. Moreover, these quantities appear to depend mainly on the averaged values of the lattice functions rather than the details of their profile. The same picture also shows $\langle |I_{xz}| \rangle_s \ll |\langle I_{xx}\rangle_s|$ or $\langle I_{zz}\rangle_s$. Because $\mathcal{H}_x \simeq 10$ cm, $\beta_x \simeq 1$ m and $\gamma_0 \simeq 50$ we conclude that on the RHS of Eq. (1) the dominant term is $\gamma_0^2 \langle \mathcal{H}_x I_{zz}\rangle_s / \varepsilon_x$.

These observations are consistent with the profiles of the IBS growth rates reported in Fig 3. Notice that while $1/\tau_x$ shows a strong correlation with $\mathcal{H}_x$ (Fig. 2), $1/\tau_z$ (*i.e.* I_{zz}) is roughly constant along the lattice except at the IP (s=0) where both β–functions become very small causing the denominator in the integrand (4) also to be small. Incidentally, in Fig. 3 also observe the reasonably good agreement between the IBS rates as calculated according to BM and Piwinsky. Because the main difference in Piwinki calculation comes from neglecting derivatives of the lattice functions the agreement suggests that the smooth approximation for the lattice we are considering may be reasonable good.

In the smooth approximation we have $\mathcal{H}_x \simeq \beta_x^3/R^2$ where R is the average radius of curvature. The expression $\tau_x^{-1} \simeq \gamma_0^2 \langle \mathcal{H}_x I_{zz}\rangle_s / \varepsilon_x = \gamma_0^2 \beta_x^3 \langle I_{zz}\rangle / (\varepsilon_x R^2)$ suggests that a way to minimize τ_x^{-1} is to decrease β_x (*i.e.* increase the tune) provided that at the same time I_{zz} does not increase too much. Indeed this is the case. As it happens, the net effect of increasing the tune is to make $1/\tau_x$ smaller and $1/\tau_z$ larger. Another way to appreciate this complementarity between horizontal and longitudinal growth rates is to recall the existence (again in the smooth approximation) of the invariant

$$\left\langle \frac{1}{\beta_x} \right\rangle_s \varepsilon_x + \left\langle \frac{1}{\beta_y} \right\rangle_s \varepsilon_y + \left(\frac{1}{\gamma_0^2} - \left\langle \frac{\mathcal{H}_x}{\beta_x} \right\rangle_s \right) \sigma_p^2 = \text{const.}, \tag{5}$$

which was first pointed out by Piwinski. [Existence of this invariant is not mentioned in the BM paper but can be easily derived from (1)-(4) after observing that $I_{xx}+I_{yy}+I_{zz} = 0$ and $I_{xz} = 0$ (the latter only holds in the smooth approximation)]. In the smooth approximation $\langle \mathcal{H}_x/\beta_x\rangle_s = 1/\nu_x^2 =$ mom. compaction. Because for $E \simeq 25$ MeV, $\nu_x \simeq 2$ we have $(1/\gamma_0^2 - 1/\nu_x^2) < 0$ (*i.e.* the machine is above transition), from (5) we deduce that an increase in σ_p results into an increase in ε_x. However, for a given increase in σ_p the growth of ε_x is less pronounced if the factor $(1/\gamma_0^2 - 1/\nu_x^2)$ is smaller in absolute value. Above transition its absolute value can be decreased by increasing the tune. This tradeoff is summarized in Fig. 6, which reports the variation of emittances and momentum spread after $t = 0.016$ sec as calculated by solving the equations for the evolution of the emittances in the smooth approximation. A similar tradeoff is also expected to apply to the nonsmooth lattice, with the difference that the function to minimize in order to keep the growth of ε_x under control is $\langle \mathcal{H}_x\rangle_s$ rather than $1/\nu_x^2$.

In conclusion, we have shown that a 0.5 m radius, 25 MeV electron storage ring can operate at a 120 Hz repetition rate with emittance degradation due to IBS of about a factor 2. An exchange between the growth in momentum spread and the horizontal emittance is possible in principle by an appropriate modification of the lattice.

This work was carried out in close collaboration with R. Loewen, A. Kabel, and R. Ruth and was supported by DOE contract DE–AC03–76SF0051.

4 REFERENCES

[1] Z. Huang and R. Ruth, Phys. Rev. Lett. 80 p. 976 (1998).

[2] J. Bjorken and S. Mtingwa, Part. Accel., **13**, 115 (1983); A. Piwinski in A. Chao and M. Tigner, *Handbook of Accelerator Physics and Engeneering*, p. 125, World Scientific, (1999).

[3] M. Venturini, Intrabeam Scattering and Wake Field Effects in Low-Emittance Electron Rings, these Proceedings.

[4] R. Dilao and R. Alves-Pires, Nonlinear Dynamics in Particle Accelerators, World Scientific, Singapore, 1996.